Frequency-selective asymmetric spin-echo EPI with parallel imaging for fast internally referenced MR Thermometry

M. N. Streicher[1], A. Schäfer[1], D. Müller[1], C. Kögler[1], E. Reimer[1], B. Dhital[1], R. Trampel[1], D. Rivera[1], A. Pampel[1], D. Ivanov[1], and R. Turner[1]
[1]Max Planck Institute for Human Cognitive and Brain Sciences, Leipzig, Germany

Introduction: The proton resonance frequency (PRF) shift MR thermometry method is inherently very sensitive to magnetic field perturbations in time [1], which may arise from field drift, shim instability, or susceptibility changes in surrounding tissue, and must be corrected to ensure accurate temperature measurements [2,3]. Chemical shift imaging, RF saturation and inversion methods can correct for magnetic field changes using a temperature-independent reference substance (e.g. fat) [4,5]. Recently, Ivanov et al. introduced an efficient frequency-selective spin-echo (SE) technique, which uses different slice-select gradient amplitudes for excitation and refocusing RF pulses, to image only the on-resonant species [6]. This SE technique can be applied to referenced PRF MR thermometry using an asymmetric EPI readout to retain phase sensitivity (Fig. 1). Images of the different chemically-shifted protons [7] are alternately acquired. We tested this novel method by temperature measurement, and by Bloch simulation of frequency selectivity and phase stability to varying B_0 and B_1^+ [8].

Fig. 1 The frequency selective phase sensitive SE sequence.

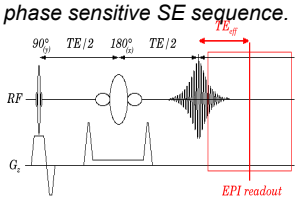

Methods: Imaging experiments were performed on a 7T whole body scanner (Siemens Healthcare, Germany) with an 8-channel head-array RF coil (RAPID Biomedical, Germany). The modified SE sequence is shown in Fig. 1. A spherical phantom (diameter 15cm), containing a mixture of 1% agar, 1% NaCl, 34% dimethyl sulfoxide (DMSO, as a internal reference) and 64% water was used for measurements. The water PRF is shifted relative to the DMSO PRF by 2ppm with a relative thermal PRF shift coefficient of α=-0.0096ppm/K [7]. An in-house-built shielded circular surface coil (10cm diameter) was placed next to the phantom parallel to the imaging slices. This coil was matched to 50Ohm with a capacitive matching network and tuned to 136.6MHz, in order to heat the phantom while mapping the temperature with the head-array coil at 297.2MHz (PRF at 7T). The heating coil was connected to a 10W RF amplifier (M68721, Mitsubishi, Japan). To heat, ca. 8W of power were applied for 50 minutes. In addition, the temperature in the phantom was monitored at two locations (4 and 7cm away from the heating coil) with fluoroptic temperature sensors (Luxtron Lumasense, USA). To achieve good separation of the two chemical species, using the same slice thickness, the excitation slice-select gradient was 23mT/m, with 5mT/m for the refocusing gradient [6]. Separate DMSO and water images were acquired automatically by alternately switching the RF-pulses to the DMSO and water PRF. Imaging parameters were: TE=25ms; k-space centred at 44ms → effective echo time TE_{eff}=19ms; TR=1s; bw=752Hz/Px; phase partial Fourier=6/8; resolution 128×128; voxel size: 1.5×1.5×1.5mm^3, GRAPPA factor 3. To correct for displacement of the water and DMSO images, due to the PRF difference, the images were co-registered using FSL [9]. The complex images of the 8 individual receive channels were subtracted from reference scans acquired at the beginning. The complex difference images were then combined to form a single image with magnitude-squared weighting, pixel-wise corrected using the smoothed DMSO images, and converted to temperature change using $\Delta T = \Delta\varphi(T)/(2\pi f_0 \alpha TE)$ where T is temperature, φ is phase, and f_0 is PRF. The B_1^+ field was mapped with the modified actual flip angle (FA) technique to assess the proper working range of this method [10]. To verify and test the frequency selectivity and phase changing effects of this modified SE sequence (Fig. 1) as a function of FA and off-resonance, we implemented a Bloch simulation using a matrix exponential approach in Matlab (MathWorks, USA) [8].

Results and Discussion: Fig. 2 and 3 show the Bloch simulation results for the frequency-selective SE sequence (Fig. 1). The dependence on the frequency offset and on the FA of the magnitude and phase of the spin echo magnetisation are displayed. As expected, the maximum signal amplitude is achieved for an on-resonant excitation FA of 90° (refocusing FA is always assumed to be twice the excitation FA) and drops off for higher and lower FA. Fig. 2 also illustrates the frequency-selectivity of the modified SE sequence. For the chosen gradient amplitudes the sequence suppresses all signal with a frequency offset (with respect to the RF-pulse frequencies) of more than ±600Hz for excitation FA up to 130°. For excitation FA above 130° the suppression is no longer reliable. Fig. 3 shows the simulated dependence of the magnetisation phase on the frequency shift and FA, at the time of the spin echo, produced by the two SE RF-pulses. Unfortunately, the phase (with respect to frequency and FA) is not flat, and varies more as FA increase. At the ideal excitation FA of 90° the highest rate of phase angle change (for offset frequencies from -300Hz to 300Hz) is -0.05°/Hz, which results in a systematic temperature error of 1.1% for an assumed effective echo time of 20ms. For an excitation FA of 130° the error could rise to 6.1%, but decreases sharply for FA below 90°. Thus, for conventional excitation FA up to 90° and B_0 inhomogeneities of less than ±300Hz this method should have very good performance.

Fig. 2

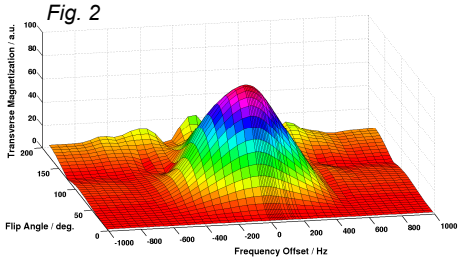

Fig. 3

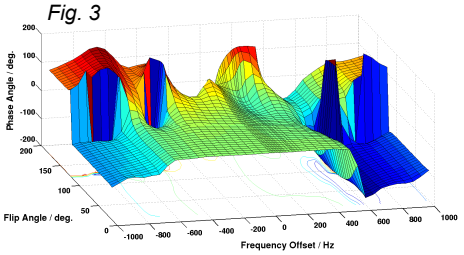

Transverse magnetisation magnitude (Fig. 2) and phase (Fig. 3) of the simulated SE sequence vs. frequency offset and FA (at time of SE). The SE sequence is frequency selective, but alters the phase.

Fig. 4

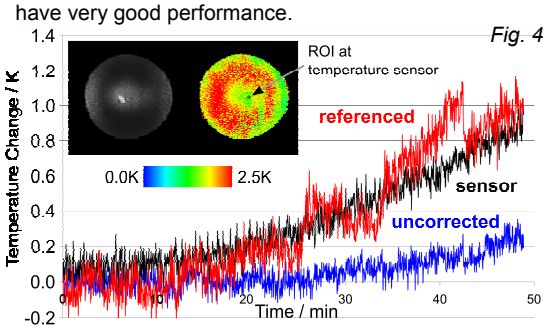

Magnitude and temperature maps after 50min RF heating and the observed heating curves. Blue - uncorrected and red - referenced MR temperature. Black – temperature reading at the displayed ROI.

Figure 4 shows the temperature evolution within the phantom during RF heating. The temperature change detected by one fluoroptic temperature sensor is shown in black. The sensor measured a maximum temperature change of (0.9±0.1)K comparing to (1.0±0.2)K for the MR thermometry ROI (red) around the probe after 50min RF heating. The MR temperature and the probe temperature deviate on average by -0.03K, with a standard deviation of 0.3K. If uncorrected, MR thermometry deviates by (0.7±0.2)K at the fluoroptic sensor tip. The other sensor (7cm away from the heating coil) measured only a small temperature increase of (0.3±0.2)K, with an average deviation of the MR temperature of –(0.1±0.2)K.

Conclusion: We have shown that this fast SE-EPI thermometry approach can compensate for any magnetic field changes up to ±300Hz, which is much greater than normally experienced field shifts. Our measurements show that PRF using an asymmetric SE and an internal reference can correct for long- and short-term B_0 field-shifts to produce high temporal and spatial resolution temperature maps with high accuracy. Thus, it is possible to detect temperature changes of much less than 1°C during RF irradiation and using parallel imaging for EPI thermometry not only reduces voxel shifts produced by temperature differences, but makes rapid water and reference substance imaging possible for field shift corrections on the order of a tenth of a second.

References: [1] Rieke V, et al, 2008, J Magn Reson Imaging, 27:376; [2] Seifert F, et al, 2007, J Magn Reson Imaging, 26:1315; [3] Grissom WA, et al, 2010, Med Phys, 37:5014; [4] Kuroda K, et al, 1997, Magn Reson Med, 38:845; [5] Taylor BA, et al, 2008, Med Phys, 35:793; [6] Ivanov D, et al, 2010, Magn Reson Med, 64:319; [7] Streicher MN, et al, 2010, ISMRM 18, #3018; [8] Allard P, et al, 1997, J Magn Reson Imaging, 129:19; [9] Smith SM, et al, 2004, NeuroImage, 23:208; [10] Amadon A, et al, 2008, ISMRM 16, #1248;